Journal Pre-proof

Active tectonics along the Cul-de-Sac - Enriquillo trough and seismic hazard for Port-au-Prince, Haiti

Newdeskarl Saint Fleur, Nathalie Feuillet, Yann Klinger
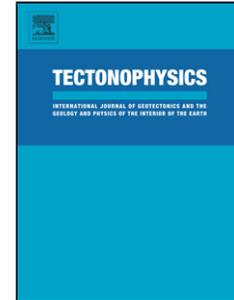
Please cite this article as: Fleur NS, Feuillet N, Klinger Y, Active tectonics along the Cul-de-Sac - Enriquillo trough and seismic hazard for Port-au-Prince, Haiti, *Tectonophysics* (2019), doi: https://doi.org/10.1016/j.tecto.2019.228235

This is a PDF file of an article that has undergone enhancements after acceptance, such as the addition of a cover page and metadata, and formatting for readability, but it is not yet the definitive version of record. This version will undergo additional copyediting, typesetting and review before it is published in its final form, but we are providing this version to give early visibility of the article. Please note that, during the production process, errors may be discovered which could affect the content, and all legal disclaimers that apply to the journal pertain.

Active tectonics along the Cul-de-Sac - Enriquillo trough and seismic hazard for Port-au-Prince, Haiti

Newdeskarl Saint Fleur[1]*, Nathalie Feuillet[1], and Yann Klinger[1]

[1]Université de Paris, Institut de Physique du Globe de Paris, CNRS, Paris, France.

*Corresponding author. Email: newdeskarl@gmail.com

Highlights

Active folding in the Cul-de-Sac–Enriquillo plain using high-resolution imagery data
Study of the current and paleo drainage systems in the Cul-de-Sac–Enriquillo plain
Offset of the paleofan of Port-au-Prince by the Enriquillo fault
Active tectonics in Port-au-Prince
Seismic hazard in Port-au-Prince

Abstract-

The active faults in Haiti were not well known and no detailed mapping of active fault traces was available before the 2010, M7.0 earthquake. The lack of detailed fault mapping hindered the interpretation of the event and the seismic hazard assessment. Here, using high-resolution LIDAR topography, aerial photographs, bathymetric charts, together with geological data complemented with field observations, we carried out a morphotectonic analysis at a variety of scales. We analyzed the drainage network at the northern front of the Massif de la Selle – Sierra de Bahoruco (MSB) by mapping the fans of the main rivers and their associated drainage basins. We found that the areas of all the fans were compatible with the sizes of their drainage basins, except the paleofan of Port-au-Prince. We interpret that this paleofan has been offset by 7.9 ± 0.3 km across the main strike-slip Enriquillo-Plantain Garden Fault (EPGF) and we estimate a

1

minimum horizontal slip rate of ~3mm/yr over the Pleistocene. Moreover, in the Cul-de-Sac – Enriquillo plain, within which the capital city of Port-au-Prince is located, we mapped numerous NW-SE to WNW-ESE-striking Quaternary folds and thrust faults. Some of the thrust faults are north-dipping and located to the southern front of the Matheux-Neiba Lower Miocene fold. Other thrusts, such as those near Ganthier, Jacquet, Nan Cadastre, and Port-au-Prince, are south-dipping and located along the northern front of the MSB Lower Miocene fold. Previously, Saint Fleur *et al.* (2015) showed that the 2010 Haiti earthquake activated both one of the young thrusts (Lamentin) and the EPGF, consistent with oblique convergence between the Caribbean and the North American plates.

1. Introduction

The northern boundary of the Caribbean plate is curved between the Lesser Antilles arc and Hispaniola (Fig. 1, inset). This curvature implies that the almost-frontal convergence between the Caribbean and the North American plates at the Lesser Antilles becomes oblique near Hispaniola [*DeMets et al.,* 2010; *Sykes et al.,* 1982]. At the longitude of Hispaniola, the plate motion is partitioned between shortening and strike-slip faulting [*Dolan et al.,* 1998]. This shortening is accommodated by several folds and thrusts located in the central part of the island and offshore [*Pubellier et al.,* 1991]. Onshore, the compression has produced mountain ranges and valleys. The mountains reach 2680 m high (Pic La Selle) in the Massif de la Selle, in Haiti, and ~3100 m high (Pico Duarte) in the Cordillera Central, in Dominican Republic (Fig. 1). The folds in the central part of Hispaniola are situated in between two major, left-lateral strike-slip faults, the Septentrional Fault (SF) to the north, and the Enriquillo-Plantain Garden Fault (EPGF) to the south.

Based on GPS data, the short-term slip rate along the SF is estimated at 9 ± 2 mm/yr [*Benford et al.*, 2012; *Manaker et al.*, 2008]. Geomorphic analysis and radiocarbon dating suggest a similar longer term slip rate between 6 and 12 mm/yr over the last 5 kyr in central Cibao Valley (Fig. 1) [*Prentice et al.*, 2003]. In the case of the EPGF, the geodetic slip rate over ~10 years, is in the range of 4 to 12 mm/yr [*Benford et al.*, 2012; *Calais et al.*, 2010; *Dixon et al.*, 1998; *Mann et al.*, 2002]. This large uncertainty is likely a result of the relatively sparse GPS network in Haiti, especially for the earlier campaigns [*Dixon et al.*, 1998]. Thereafter, the slip rate was estimated at 6 ± 2 mm/yr [*Symithe and Calais*, 2016]. In addition to this left-lateral slip, 5.7 ± 1 mm/yr of shortening is estimated, using GPS data, in the vicinity of the EPGF. This shortening may be accommodated by the fold and thrust belt bordering the main strike-slip EPGF (Fig. 2) [*Benford et al.*, 2012]. We interpret that the deformation is mainly compressional at the northern front of the Massif de la Selle and Bahoruco Mountains. Because ground shaking associated with thrust faults may be twice that associated with strike-slip faults, these compressional structures imply greater seismic hazard than previously recognized [*Symithe and Calais*, 2016].

3
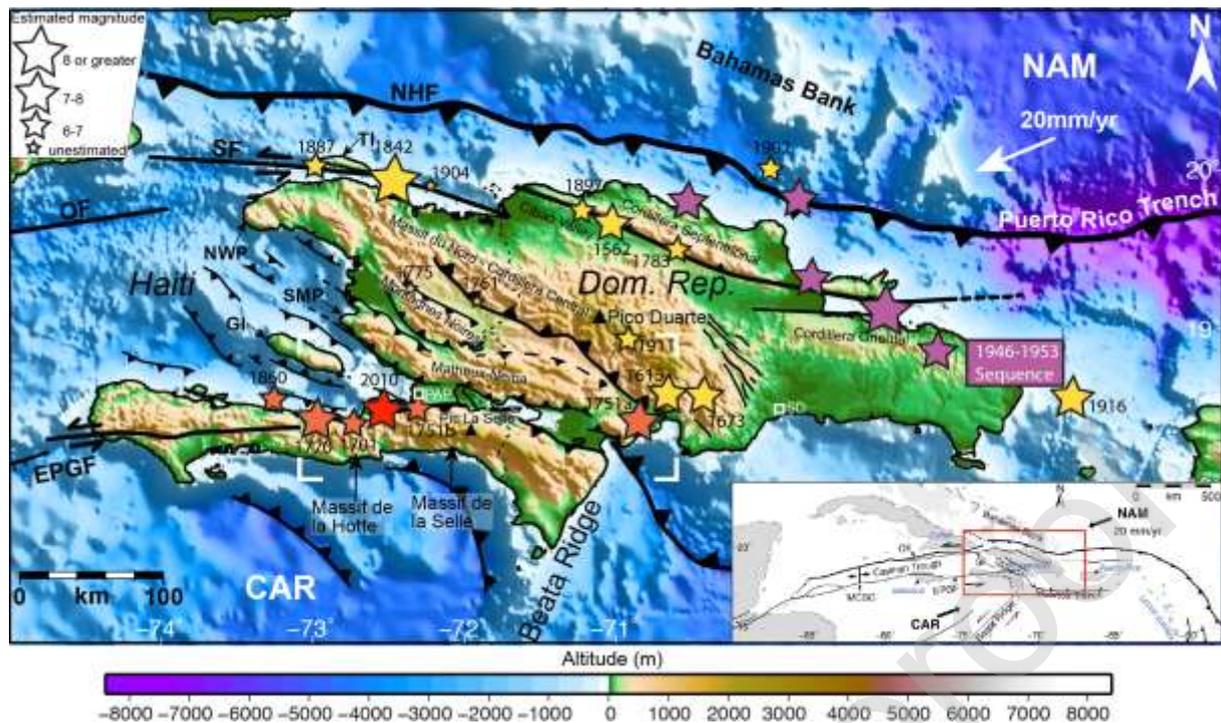
Figure 1: Tectonic setting and historical seismicity of Hispaniola. The hyper oblique convergence of 20 mm/yr (white arrow) between North American (NAM) and Caribbean (CAR) plates is partitioned into 1) two main strike-slip faults : the Septentrional Fault (SF) to the north and the Enriquillo-Plantain Garden Fault (EPGF) to the south; and 2) numerous thrust faults forming the Trans-Haitian Belt. This map is obtained using 1) bathymetric and topographic data: SRTM 30+ (pixel : 900 m) illuminated from the northeast; 2) bathymetric chart (1/25000) from the Service Hydrographique et Océanographique de la Marine (SHOM); 3) seismic profiles from Mann *et al.* (1995); 4) LIDAR data (pixel 1 m), and 5) geological maps of Hispaniola [e.g., *Momplaisir and Boisson,* 1988; *Toloczyki and Ramirez,* 1991]. The stars denote the historical seismicity. The northern and central seismicity (yellow and purple) is from the NOAA database; and the southern seismicity (orange) is from Bakun *et al.* [2012]. The 2010 earthquake is evidenced in red. The white box is the location of Fig. 2. OF : Oriente Fault ; NHF : Northern Hispaniola Fault ; TI : Tortue Island ; NWP : Northwestern Peninsula ; SMP : Saint-Marc Peinisula ; GI : Gonâve Island ; PAP : Port-au-Prince; SD : Santo Domingo.   Inset : Tectonic setting of the Northern Caribbean. Main tectonic structures are from Feuillet (2000). MCSC : Mid-Cayman Spreading Center. The ~N70°E convergence direction between Caribbean and North American Plates is from Sykes *et al.* (1982). The red box locates the main map.

Along the southern Haitian peninsula, historical earthquakes occurred (Fig. 1) in 1701, 1751 and 1770, causing severe damage in Port-au-Prince [*de St. Méry,* 1803]. On 8 April 1860, a tsunamigenic earthquake occurred in southern Haiti that produced waves observed at Anse-à-Veau and Miragoâne [*Bakun et al.,* 2012]. Most earthquakes of the 18th century are generally attributed to the EPGF [e.g., *Ali et al.,* 2008; *Bakun et al.,* 2012; *McCann,* 2006]. The 2010 earthquake occurred in the immediate vicinity of EPGF [e.g., *Saint Fleur et al.,* 2015; *Douilly et al.,* 2013; *Symithe et al.,* 2013], and included both strike-slip and reverse motion. Most aftershocks were associated with thrust mechanisms [*Mercier de Lépinay et al.,* 2011; *Nettles and Hjörleifsdóttir,* 2010], which, along with coastal uplift indicate that this earthquake activated a thrust fault along the southern peninsula, near Port-au-Prince [*Hayes et al.,* 2010; *Calais et al.,* 2010; *Prentice et al.,* 2010]. Despite its large magnitude, no significant surface rupture occurred along the EPGF [e.g., *Bilham,* 2010; *Lacassin et al.,* 2013; *Prentice et al.,* 2010]. For this study, we carried out a morphotectonic analysis in southern Haiti for a better understanding of this earthquake and conducted detailed fault mapping in the Cul-de-Sac – Enriquillo trough for future seismic hazard assessment in the area. We conducted our fault mapping at several scales, using LIDAR topography (pixel 1 m), aerial photographs (pixel 0.3 m), and bathymetric charts (scale: 1/25000), complemented with field observations and local geological data. This is the first large scale seismotectonic map presented for southern Haiti. Finally, on the basis of our detailed fault mapping, we discuss the implications for seismic hazard near significant cities such as Port-au-Prince, Pétion-Ville, and Carrefour.

5
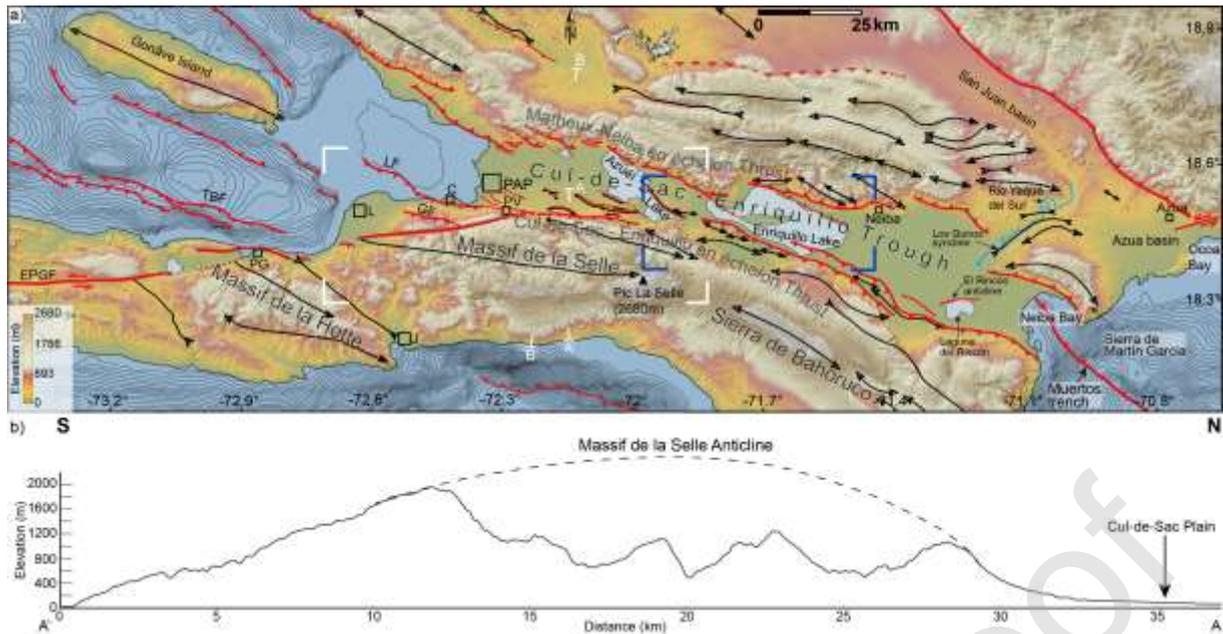
Figure 2: a) Tectonic map of southeastern Hispaniola. This map mainly evidences the Cul-de-Sac – Enriquillo trough bounded by two giant fold systems: the Matheux-Neiba and the Massif de la Selle-Sierra de Bahoruco folds. In the Cul-de-Sac – Enriquillo trough itself, numerous young folds are emerging and connected to the older Matheux-Neiba and to the Massif de la Selle-Sierra de Bahoruco fold systems. The folds and thrusts are oriented NW-SE to WNW-ESE. This orientation tends to be disturbed eastward. Fold axes are from Mann *et al.* (1991, 1995) and this study. White and blue boxes are locations of Fig. 3 and 6, respectively. AA' locates b); BB' locates Fig. 15b. Topographic data: ASTER (pixel 30 m); Bathymetric data: SRTM 30+ (pixel 900 m), isobaths are 100 m interval. EPGF: Enriquillo-Plantain Garden Fault; TBF: Trois-Baies Fault; LF: Lamentin Fault; GF: Gressier fault; L: Léogâne; J: Jacmel; PAP: Port-au-Prince; PV: Pétion-Ville; C: Carrefour; PG: Pétit-Goâve. b) Topographic profile showing the Massif de la Selle Anticline. The two flanks of the anticline have different morphology. The northern flank is steeper.

2. Overall tectonic setting of Southern Haiti

Using magnetic data, Pindell *et al.* (1988) suggested that the EPGF initiated in the middle Eocene, propagating eastward from the Mid-Cayman Spreading Center (Fig. 1, inset). The fault seems to have reached the southern peninsula of Haiti in Pliocene time, disrupting Late Miocene terranes [*Calais and Mercier de Lépinay,* 1995; *Calmus,* 1983; *Calmus and Vila,*

1988; *Cooper,* 1983; *Heubeck and Mann,* 1991a; b; *Mann et al.,* 1984; *Van Den Berghe,* 1983; *van den Bold,* 1975]. The 1100 km-long EPGF crosses the southern peninsula of Haiti in a N85°E direction.

The morphology of Hispaniola consists of several NW-SE to WNW-ESE subparallel anticlines separated by several kilometer-wide valleys likely related to ramp basins [*Mann et al.,* 1991]. One of the largest of these valleys is the Cul-de-Sac − Enriquillo plain or trough (CSE) (Fig. 2a). This basin is bounded to the north by the N100-120°E, ~205 km long, ~25 km wide Matheux − Neiba en échelon thrust system and to the south by the N100-130°E, ~180 km long, ~40-50 km wide Massif de la Selle - Sierra de Bahoruco (MSB) northward verging Fold and thrust belt [*Saint Fleur et al.,* 2015] of Miocene age. The region is underlain by Eocene to Miocene limestones that overlie a Campanian-Maastrichtian tholeitic complex (basalt). The Massif de la Selle anticline is asymmetric with a southern flank that is 12 km wide and dips southward ~18° from 2000 m of elevation to sea level (Fig. 2b). This structural surface is well preserved and only incised by small rivers. Consequently, along the southern coast, the alluvial deposits are small and are only visible at large scale. The northern flank of the anticline is steeper than the southern flank, with about ~800 m of relief over only 3 km.

3. Drainage network analysis and offset of the EPGF in Port-au-Prince

In contrast to the southern flank of the Massif de la Selle anticline, the northern flank is incised by a dense drainage network of significant north-flowing rivers (e.g., Momance river, Grise river) (Fig. 3a). These rivers flow either to the bay of Port-au-Prince or to Azuéï lake, and have deposited large alluvial fans along the northern piedmont of the Massif de la Selle. From east to west, these alluvial fans are mainly the fans of Fond Parisien, Blanche, Grise, Froide, and Momance rivers, and the Port-au-Prince fan.

7
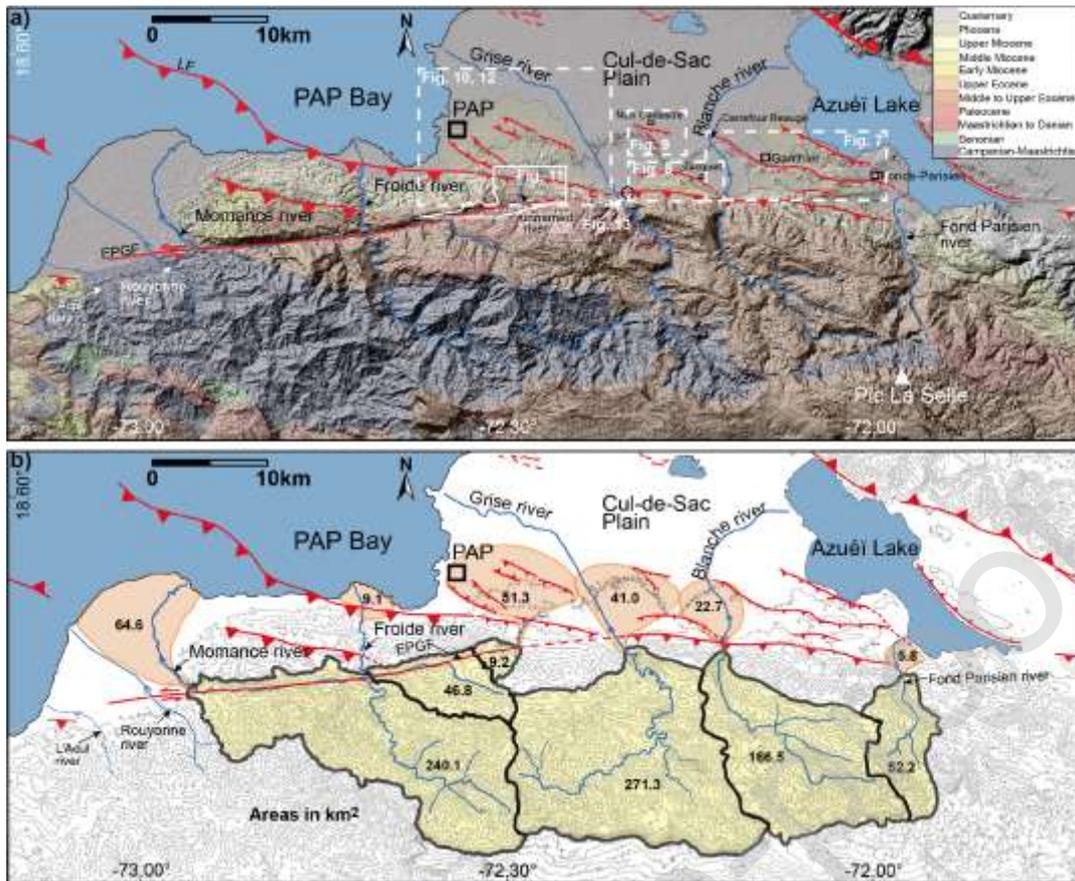
Figure 3: a) The Cul-de-Sac Plio-Quaternary folds and thrusts that disturb the gentle topography of the plain. Topographic data: ASTER (pixel: 30 m). Contours are 50-m interval. The geological map overlain on the topographic data has been redrawn from the original map of Momplaisir and Boisson (1988). Note the locations of Fig. 7-12. PAP: Port-au-Prince; LF: Lamentin Fault. b) Map of the alluvial fans (shaded orange) of the northern piedmont of the Massif de la Selle, including the paleofan of Port-au-Prince, with respect to their related catchments or drainage basins (shaded yellow). On the map, the paleofan of Port-au-Prince, compared to the other fans, is abnormally too big (~51.3 km^2) with respect to its catchment (9.2 km^2). The latter catchment does not correspond to the one that should have generated the paleofan. This pattern may evidence the offset of the paleofan by the Enriquillo-Plantain Garden Fault (EPGF). Values are areas in km^2. Once the mapping was done, the area values were obtained using the measurement tools of ArcGIS. PAP: Port-au-Prince. Topographic data: ASTER (pixel: 30 m); contours: 100-m interval.

The Grise river, which is about 60 km long, is the most prominent river that crosses the Cul-de-Sac plain (Fig. 3). The river's source is in the Paleogene carbonates of the northern flank of the Massif de la Selle anticline, and most of the drainage area is within the Campanian-

9

Maastrichtian basalt unit exposed at the crest of the anticline. The river meanders over about half of its length, along its upstream and then flows in a roughly straight, ~N150°E direction for ~12 km through the Cul-de-Sac plain. Finally, it changes course to N115±20°E and bounds northern Port-au-Prince before flowing into the bay of Port-au-Prince. This configuration suggests that the paleofan of Port-au-Prince creates sufficient topography to force the Grise river to flow around it.

The drainage basin of Grise river has a total area of 271.3 km^2 and is the largest of the Massif de la Selle. The southern boundary of the drainage basin is close to the geological contact between the tholeitic complex of the anticlinal crest and the Eocene limestone of the southern flank of the anticline (Fig. 3). Immediately above the contact the limestone forms a cliff that is 630 to 1070 m high (Supplementary Fig. S1) and more than 20 km long. The Grise river fan is ~41 km^2 in area and is located where the river flows out of the Massif de la Selle into the Cul-de-Sac plain (Fig. 3b).

3.1. Offset of the Paleofan of Port-au-Prince

The densely populated city of Port-au-Prince (PaP) is located at the western edge of the Cul-de-Sac plain. It is built on a paleofan, which we refer to as the PaP paleofan, and on surrounding alluvial deposits. The EPGF is located immediately south of the PaP paleofan. We identified an unnamed river that flows N80°E along the EPGF and abruptly changes direction to N45°E at the apex of the PaP paleofan where it crosses the fault and flows along the southeastern edge of the fan (Fig. 3 and 11). The source of the unnamed river is in the Paleogene carbonate rocks of the northern flank of the Massif de la Selle and is fed by a small catchment of 9.2 km^2.

Most of the large fans shown in Figure 3b correspond to large drainage basins, consistent with numerous studies carried out in different climatic, lithologic and tectonic contexts [e.g., *Bull,* 1962; *Bull,* 1977; *Fraser and DeCelles,* 1992; *Giles,* 2010; *Guérit,* 2014; *Harvey,* 1997; *Mather et al.,* 2000; *Weissmann and Fogg,* 1999; *Whipple and Trayler,* 1996]. However, an exception is the large PaP paleofan (51.3 km^2), which is situated in front of the small catchment (9.2 km^2) of the unnamed river. Following Bull [1962; 1977], we plot our drainage areas as a function of their associated fan areas (Fig. 4). The PaP paleofan is clearly an outlier, and we therefore exclude it in our initial analysis. The five points (in green) are well correlated (black heavy line). In this case, the PaP paleofan, shown in red, plots significantly below the trend. When we include it in the fit (grey dotted line), the five green points are less well correlated because the fit is influenced by the paleofan. But, the PaP paleofan still does not lie near the trend. Thus, we conclude that the drainage basin of the unnamed river that is currently in front of the paleofan is too small be the original source of this fan. We propose that the Grise river, because of its size and location, is the original source of the paleofan, and that the PaP paleofan has been left-laterally offset across the EPGF.

11
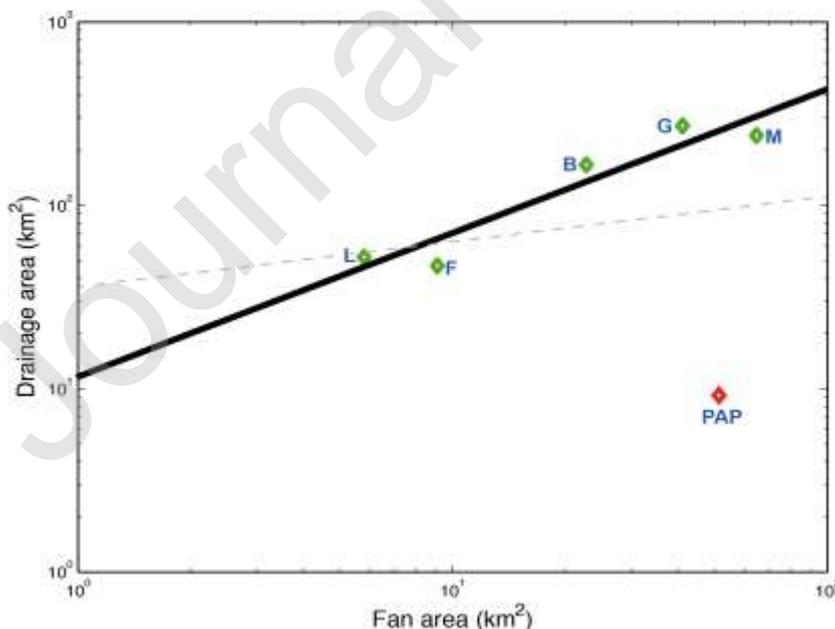
Figure 4: Plot showing correlation between fan areas and drainage areas. The green points are for the fans that relatively follow the correlation. The Port-au-Prince paleofan (red point) does not follow the correlation law between its present-day area and its drainage area. The black heavy line is the regression line for the five green points alone. The grey dotted line is the regression line when the paleofan of Port-au-Prince is included in the fit. In both cases, the paleofan is out of the tendency. L: the fan of Lèwòch river or Fond Parisien river; B: the fan of Blanche river; G: the fan of Grise river; PAP: Port-au-Prince paleofan; F: the fan of Froide river; M: the fan of Momance river.

3.1.2.- Tectonic reconstruction of the paleofan of Port-au-Prince

In order to estimate the amount of offset, we first overlay the detailed geological map of Port-au-Prince area [*Cox et al.,* 2011] on a shaded ASTER DEM (pixel: 30 m) (Fig. 5a). We then reconstruct the paleofan by moving it eastward with respect to the EPGF in order to estimate its original position in front of the present-day Grise river. Between Pétion-Ville and Dumay (western bank of Grise river), the EPGF trace is poorly expressed geomorphically. A fault zone is exposed near Dumay in the eastern bank of Grise river where several of the exposed fault strands have a component of reverse displacement (Fig. 13). We refer to these reverse faults as the Dumay Fault zone, and suggest that it may be independent of the EPGF. If this interpretation is correct, and the EPGF continues eastward with the same azimuth as in the Léogâne – Pétion-Ville section, we estimate that the paleofan is offset 9 ± 0.5 km (Supplementary S2). We estimate the uncertainty based on the sweep angle of the river. In the past, the river could have flowed along the eastern edge of the valley, yielding a maximum offset of 9.5 km, or along the western rim, yielding a minimum offset of 8.5 km. If, instead of projecting the EPGF N80°E from Pétion-Ville we project it to the exposure of the Dumay Fault in the eastern cutbank of the Grise river, we find the same offset of 9 ± 0.5 km (Supplementary S2). For these two scenarios, we projected the upstream course of the Grise river to the apex of the reconstructed paleofan perpendicular to the fault trace. An alternative reconstruction is to use the overall NW-SE orientation of the Grise river to project the river to apex of the

paleofan. In this case, using the same sweep angle criterion, we obtained a maximum offset of 8.2 km and a minimum one of 7.6 km by projecting the eastern and the western edges of the Grise river valley, respectively, to the apex of the paleofan. If instead, we use the orientation of the present-day active riverbed to project the river to the apex of the paleofan (Fig. 5b), we find an offset of 7.9 km. Because the 7.9 km reconstruction also brings the offset Froide river into alignment, we consider 7.9 km to be our best solution (Fig. 5).
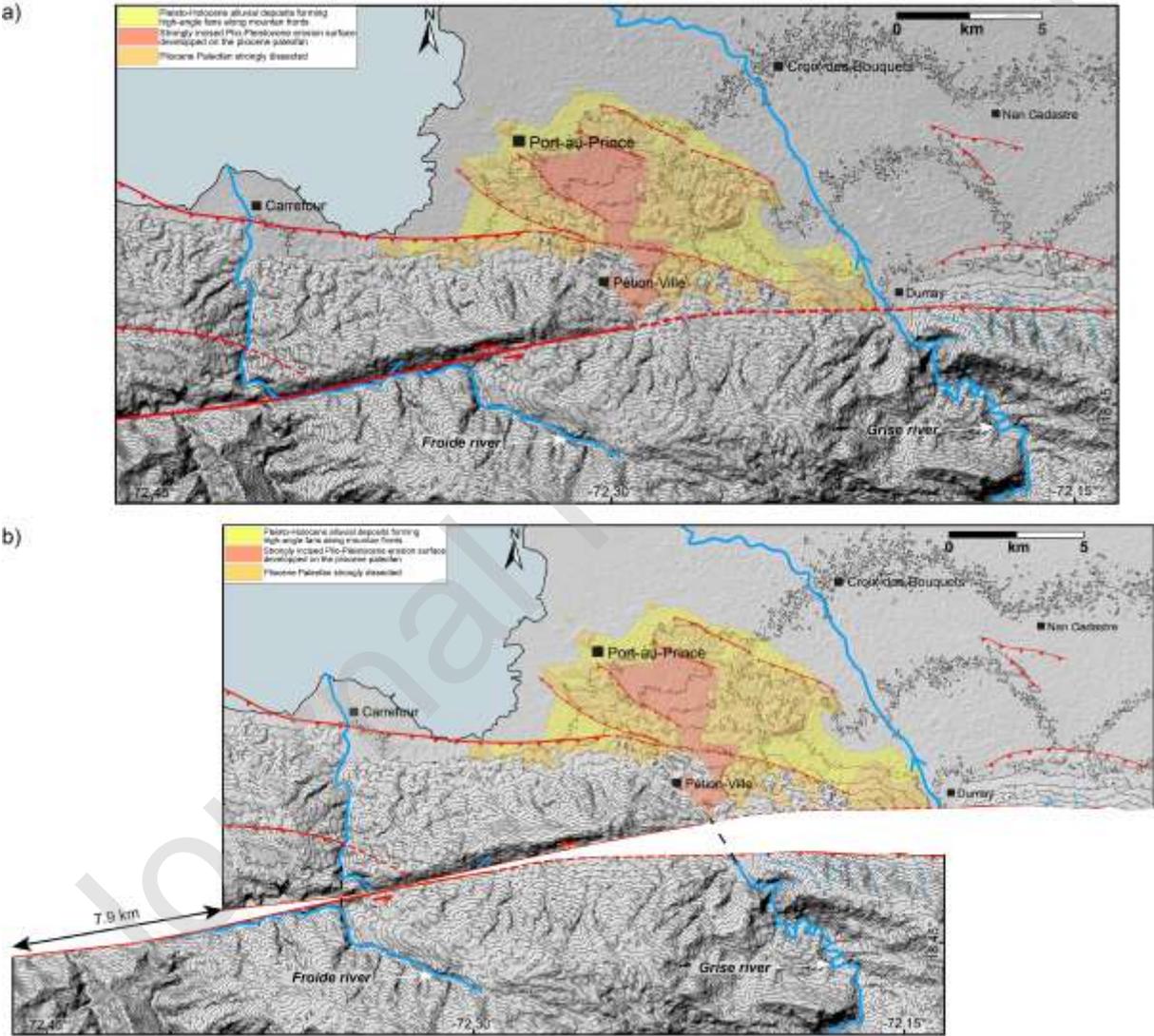
Figure 5: a) The paleofan of Port-au-Prince between Froide and Grise rivers. The Grise river is, by its position, the best candidate to have generated the paleofan. Topographic data: ASTER (pixel: 30 m). Contours are 50 m interval. Geological information is from Cox *et al.* (2011). b) Tectonic reconstruction of the paleofan of Port-au-Prince. The

13

paleofan has been displaced by 7.9±0.3 km (see text for discussion). This reconstruction also enables us to reconstruct the course of the Froide river.

4. Active thrusting in the Cul-de-Sac – Enriquillo plain

The CSE is a set of basins that encompasses the Cul-de-Sac plain and the Enriquillo valley. The CSE is separated from the Azua basin by the Sierra de Martín Garcia (Fig. 2a). The entire CSE extends from the bay of Port-au-Prince to the bay of Neiba. It is 135 km long and up to 25 km wide and bounded by mountains to the north and south.

The CSE plain is relatively flat (no higher than a few tens of meters) and is underlain by Pliocene-Quaternary fluvial and marine sediments [*Mann et al.,* 1991; *Taylor et al.,* 1985]. Near the southern edge of the CSE is a series of ~N115°E elongate low hills that are underlain by folded sediments and have been interpreted as being the surface expression of young anticlines (Fig. 6) (*Briggs et al.,* 2012; This study). The flat topography of the CSE is thus disturbed by active folding mostly associated with blind thrust faults.
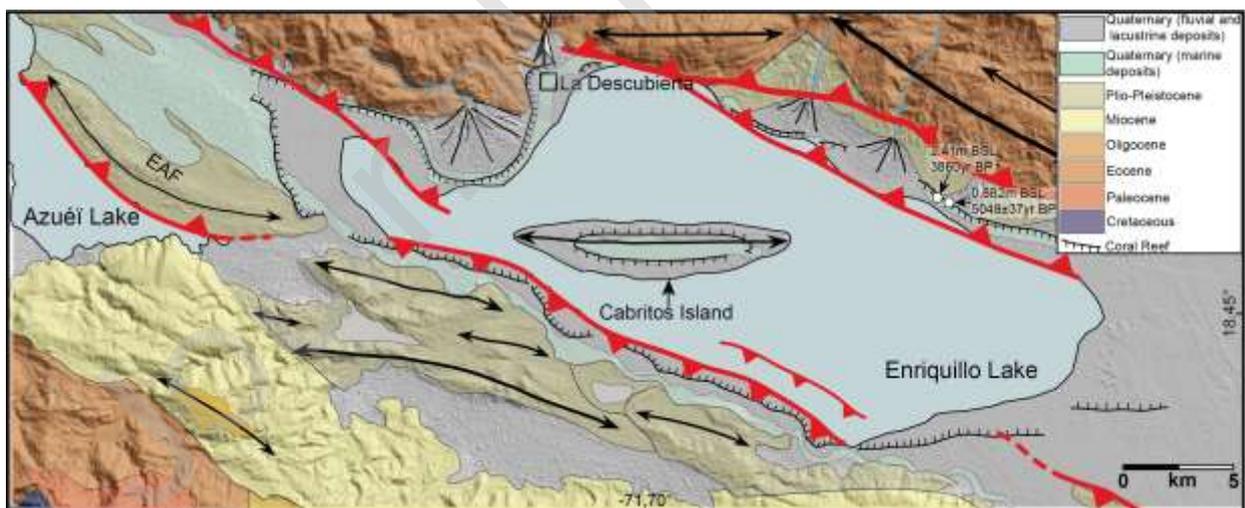
Figure 6: Morphotectonic map of the Enriquillo Lake area revisited from Mann *et al.* (1995). The lake is bounded by Plio-Quaternary folds and coral reefs. White-filled circles are uplifted coral reefs sampled and dated by Taylor *et al.* (1985) and Mann *et al.* (1995). Topographic data: ASTER (pixel: 30 m); geologic contacts are redrawn from

the 1/250000 geological maps of Haiti and Dominican Republic [*Toloczyki and Ramirez, 1991*]. EAF: Eastern

Azuéï Fold.

4.1. The area of the Enriquillo Lake

Enriquillo Lake lies within the Enriquillo Valley in the eastern part of the CSE. The lake is ~40 km long and ~12 km wide, with its long axis oriented N105°E (Fig. 6). The lake is below sea level (-42 m), and this part of the CSE experienced a marine transgression about 10 kyr ago [*Taylor et al., 1985*]. The E-W-striking, ~12 km long and less than 2 km wide Cabritos Island lies in the middle of the lake. This elongate island is bordered by fossil coral reefs that are uplifted, probably due to active folding [*Mann et al., 1995*]. Mobil multichannel seismic data acquired to the east of Cabritos Island show that the lacustrine sediments are folded, indicating that the Cabritos anticline continues below the lake [*Mann et al., 1995*]. Fossil Holocene coral reefs were also identified and mapped around the periphery of the lake, and record Holocene eustatic variations of sea level [*Mann et al., 1995*; *Taylor et al., 1985*]. Fossil reefs are uplifted in two locations (Fig. 6) and indicate uplift at a rate of 0.5 mm/yr over the last ~5 kyr [*Mann et al., 1995*]. To the west of Enriquillo Lake, we observe an arc-shaped fold (Fig. 6). This fold, which we call the Eastern Azuéï Fold (EAF), appears to control the morphology of the eastern border of Azuéï Lake, which is oriented ~N135°E, ~25 km long and up to 10 km wide. The fold is oriented N120 ± 15°E (Fig. 6) and deforms Plio-Quaternary fluvial, lacustrine, and marine deposits. The fold is ~15 km long, ~7 km wide and up to 185 m high above sea level between the Azuéï and Enriquillo lakes (Supplementary Fig. S3).

15

In this area, additional young folds and thrusts are found along the northern margin of the Sierra de Bahoruco [*Mann et al.,* 1991; and detailed mapping in this study], and in the Cul-de-Sac plain along the northern margin of the Massif de la Selle (Fig. 7).

Figure 7: a) and b) Aerial photograph (pixel: 30 cm resized into 15 m) and interpretation of the Ganthier Fold area showing two distinct parts: a western one (dark yellow) exhibiting a youthful morphology and an eroded older eastern one (orange). Dating of the ponded sediments is from Briggs *et al.* (2012). The activity of the fold appears to have diverted the Blanche river several times. Note also the Balan Fold to the north along the western border of the Azuéï Lake. c) and d) Field photographs of the eastern wall of the Bois Galette river showing the folded interbedded lacustrine and fluvial deposits (see (b) for location). In this area, the layers dip ~33° to the north.

4.2.- Ganthier and Balan Folds and Thrusts

The ~N115°E Ganthier fold zone is one of the most significant folds in the Cul-de-Sac plain. It is ~15-km long, 1-2 km wide and ~200 m high. It extends between Carrefour Beaugé and Fonds-Parisien (Fig. 3 and 7). Figure 7a is a mosaic of aerial photographs (pixel: 30 cm resized into 15 m) showing the Ganthier fold zone incised by rivers and gullies. The eastern part of the fold zone exposes Pliocene marine marly sediments and the western part exposes tilted Quaternary fluvial sediments (Fig. 7b, 7c and 7d). In the eastern part, the Pliocene marl is exposed and eroded at the top of the fold. The Quaternary sediments are exposed along the flanks of the fold and are less eroded. The fold zone is crosscut by a series of north-flowing rivers, including the Bois Galette river (18.528840°/-72.078400°). In the field, we observed that this river, where it crosses the fold, is incised into unconsolidated, interbedded conglomerates and fine sediments oriented N138°E and dipping 33°N (Fig. 7c, d). In an unnamed drainage about 2 km west of Ganthier (and ~1 km west of Bois Galette), charcoal from a 10 m-thick section of interbedded fluvial and ponded lacustrine sediments yielded a calibrated radiocarbon age of 4978 ± 158 cal. yr B.P. [*Briggs et al.*, 2012].

North of the Ganthier fold zone, we observe that the plain adjacent to the fold is "wrinkly" over a ~10 km-long, ~2 km-wide band (Fig. 7a, b). This subtle topography is characterized by numerous dry incisions along the western shore of the Azuéï Lake. The incisions may be due to intermittent streams and thus have water when it rains. Following the slopes, some of the channels flow northeastward into the Azuéï Lake, others flow southwestward into the plain. We remark that each northeast-flowing drainage faces a

17

southwest-flowing one. These drainages might have used to flow one side (northeastward). And by tectonic uplift, the upstream might be cut from its downstream and now flow to the opposite sense (southwestward). This drainage reversal leaves wind gaps between the two branches. Thus, the whole topographic "band" undergoes active folding (the Balan Fold). The described mechanism corresponds to a classical effect of anticlinal folding as studied elsewhere [e.g., *Hubert-Ferrari et al.*, 2007].

4.3.- Jacquet Fold and Thrust

On the LIDAR data we see that the topography of the Cul-de-Sac plain is disturbed by the Jacquet arc-shaped fold (Fig. 8a). The fold is oriented N105±20°E. It is ~7 km long, 0.1-1.5 km wide and up to 260 m high. The width and the altitude of the Jacquet Fold decrease westward. This fold has a morphology similar to the other young folds in the Cul-de-Sac alluvial plain, and dipping Upper Miocene limestone beds are exposed in the eastern part of the fold (Fig. 8b). In the central part of the fold we mapped ponded sediments and several active, entrenched channels associated with alluvial terraces, suggesting Late Quaternary folding.
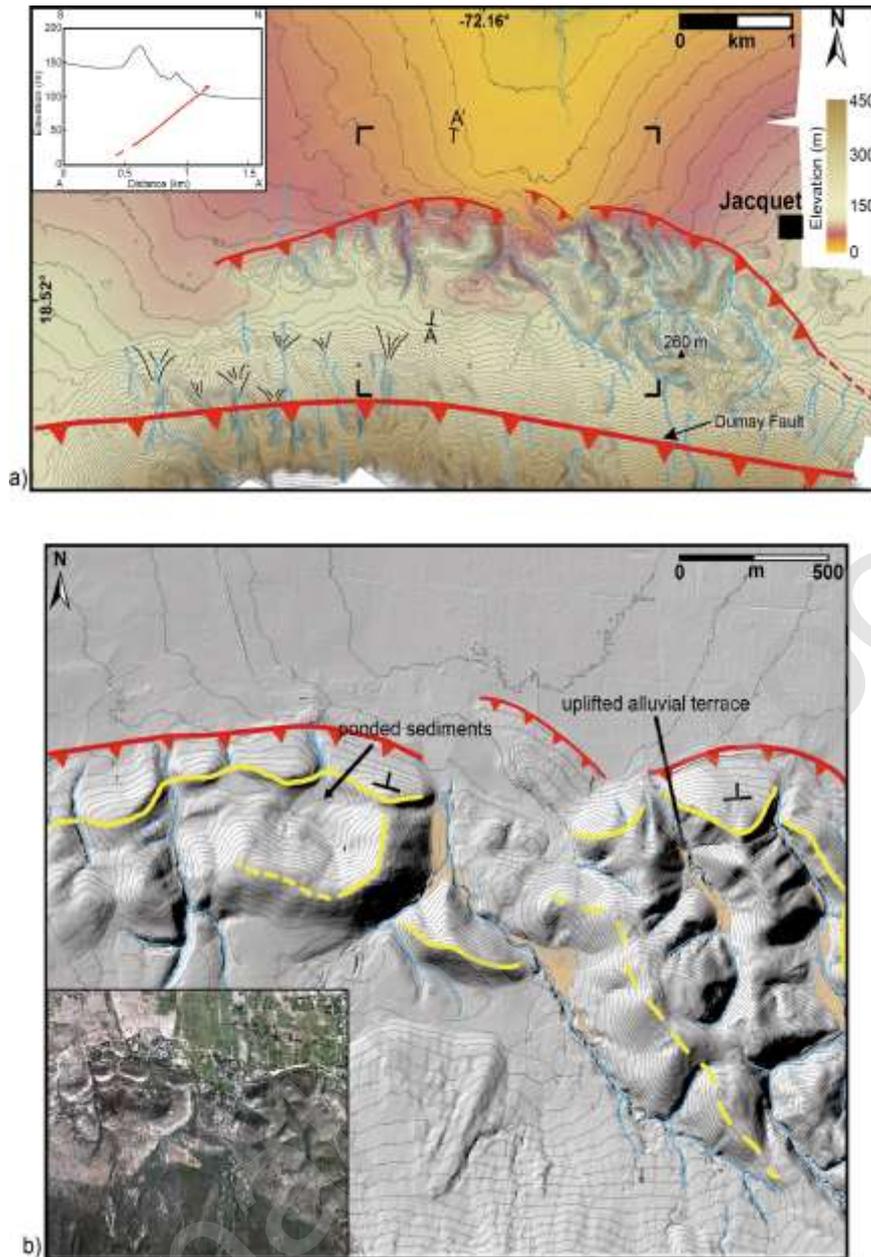
Figure 8: a) LIDAR (pixel: 1 m) topographic map of the Jacquet fold. Black box is the location of b). Inset shows a topographic profile (AA') across the fold zone. The value of the fault dip is arbitrary. b) Zoom showing numerous entrenched streams in the fold. Orange shaded areas are alluvial terraces. Contours are 5 m interval. Yellow lines are Upper Miocene beds. Inset: the same area on aerial photograph (pixel: 30 cm) offering a better resolution for the observation of the Upper Miocene outcrops.

4.4.- Nan Cadastre Fold and Thrust

19

We used the high-resolution LiDAR DEM to map another young fold that we refer to as the Nan Cadastre Fold [*Saint Fleur et al.,* 2015] (Fig. 9 and S4). It is located in the center of the Cul-de-Sac plain, between Grise river (west) and Blanche river (east) and bounded to the north by the Nan Cadastre Village (Fig. 9). The area is characterized by low hills ~80 m high. The Nan Cadastre Fold is among the smallest fold zones in the Cul-de-Sac plain. It is ~4 km long and 0.5-1 km wide. It is also located ~5 km from the Ganthier Fold and may prolongate it west-northwestward. The fold zone is divided into 2 main branches: a northern one and a southern one underlain by folds oriented N110-115°E and N130°E, respectively. We interpret that the folds are related to an emergent thrust ramp rooted on a south-dipping, low-angle, shallow décollement which splays from the master high-angle ramp located under the higher relief of the Massif de la Selle – Sierra de Bahoruco anticline (Fig. 9, inset) [*Saint Fleur et al.,* 2015].
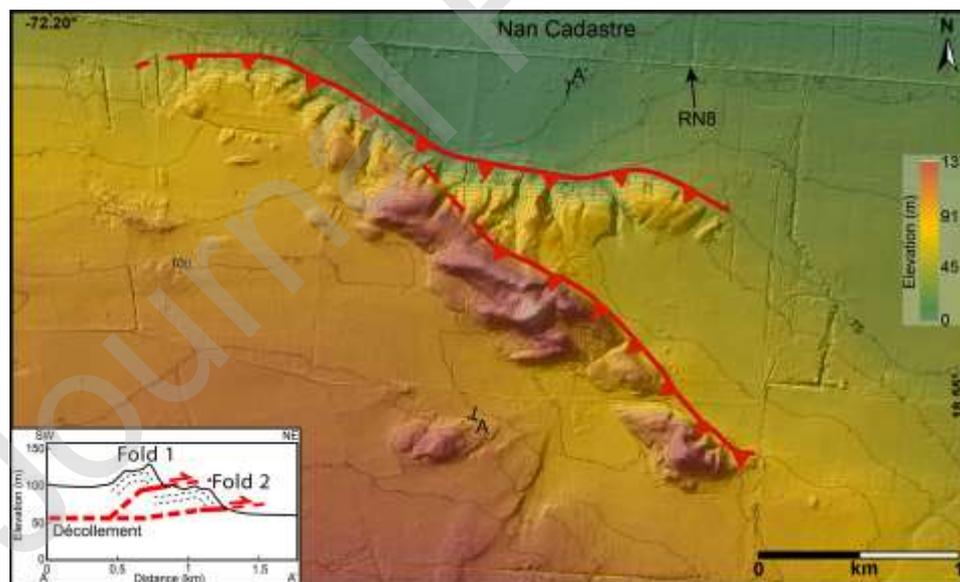
Figure 9: The area of the Nan Cadastre Fold. LIDAR (pixel: 1 m) of the area showing that the fold deforms the northern front of the fan of Grise river. RN8: National Road # 8. Contours are 5 m interval. Inset is a SW-NE

topographic profile (AA') showing the morphology of the two branches of the fold and our interpretation of the geometry of the associated thrusts (see text for details).

4.5.- Thrusting of the paleofan of Port-au-Prince

The PaP paleofan spans from Pétion-Ville (south) to the Aéroport Toussaint Louverture (north), and from Boulevard Jean-Jacques Dessalines (west) to Boulevard 15 octobre (east) (Fig. 10a). Within the fan are two parallel, 5-6 km long, 1-3 km wide, N125°E elongate hill ranges underlain by Pliocene fanglomerates. The hills are deeply eroded and incised by numerous streams and rills and reach elevation of ~300 m. The hills are about 50-100 m higher than the adjacent areas of the paleofan, which are Quaternary in age [*Cox et al.,* 2011] (Fig. 10b).

In the middle of the paleofan, between the two Pliocene hill ranges, Cox *et al.,* (2011) mapped a Plio-Pleistocene erosion surface that we interpret as an inset alluvial fan (Fig. 10a). This Plio-Pleistocene alluvial fan continues to the south until the apex of the overall paleofan. This inset fan is less eroded and less deeply incised than are the Pliocene hill ranges, supporting the interpretation that it is younger. Furthermore, the fact that the Plio-Pleistocene fan does not continue until the northern front of the Pliocene deposits may suggest that they were not emplaced simultaneously. Also, the Plio-Pleistocene fan is developed on the Pliocene paleofan, thus it is not the result of progradation of the whole paleofan. We divide the Plio-Pleistocene surface into three sub-fans: a southernmost one (SF1) in the town of Pétion-Ville, a central one (SF2), and a northern one (SF3) (Fig. 10a and 11). The southernmost sub-fan, SF1 is about 1-km long and up to ~2 km wide. It abuts against Mio-Pliocene rocks and only extends to the north within a relatively narrow space of ~0.4 km wide between the Mio-Pliocene rocks to the

21

west and a vestige of the Pliocene paleofan to the east. At this place, SF1 is deeply incised, suggesting that the stream was forced to flow through this narrow gap. At the same time, the middle of the pre-mentioned narrow space corresponds to the apex of the central sub-fan, SF2. SF2 is ~1.6 km long and up to ~1.3 km wide and is more incised than SF1. SF2 abuts against the southwestern edge of the eastern Pliocene hill range and continues to the west along a narrow space of ~0.7 km wide. Similarly to SF2, the middle of the latter narrow space acts as the apex of SF3. SF3 has about the same degree of incision as SF2, and is ~2.2 km long and up to ~3 km wide.
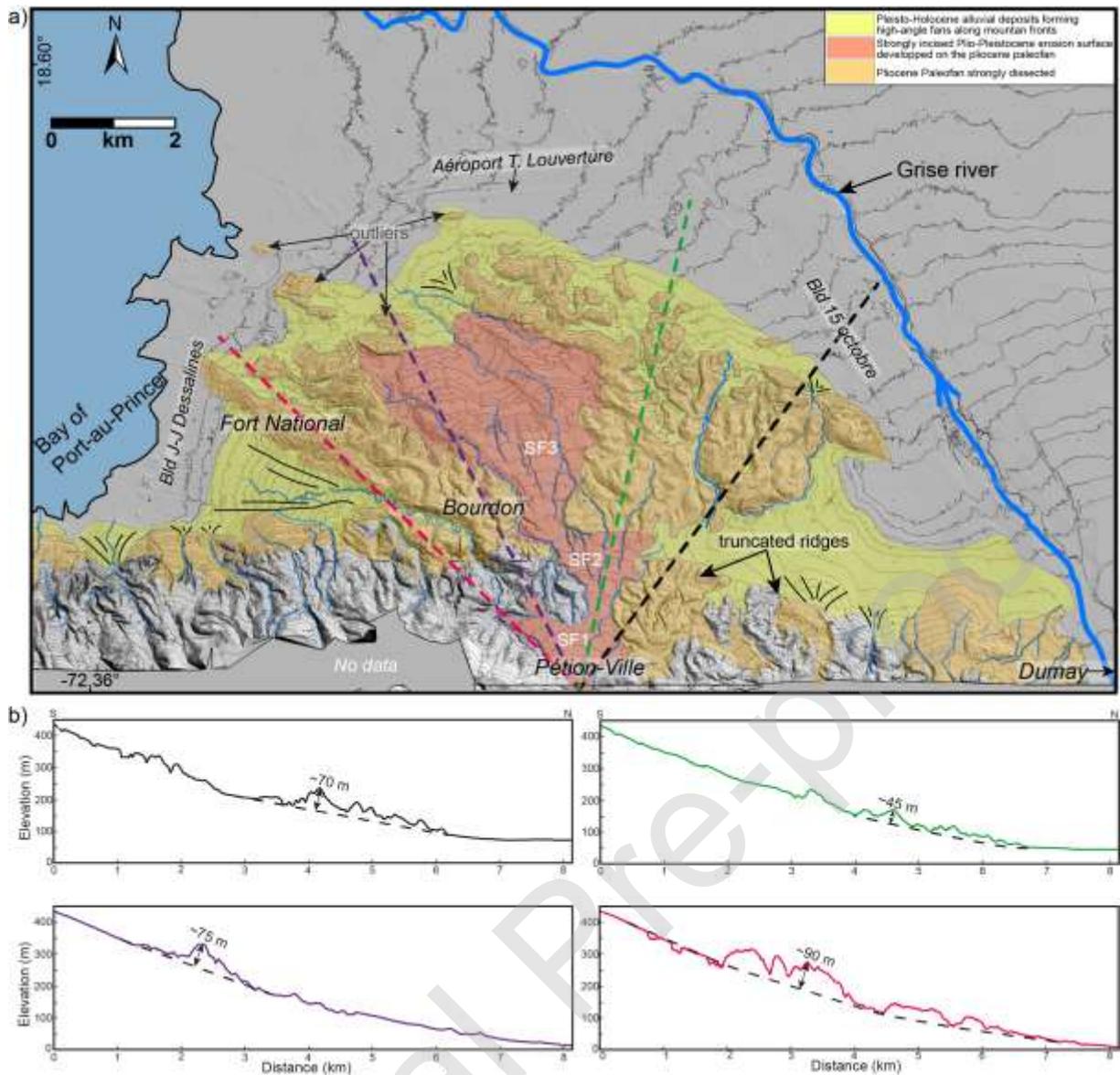
Figure 10: a) Geologic map of the paleofan of Port-au-Prince. The paleofan is mainly made of an eroded Pliocene alluvial sediment layer on which are deposed younger alluvial fans (e.g., Plio-Pleistocene). The geologic contacts are modified from Cox *et al.* (2011). Topographic contour interval is 10 m. Topographic data: LIDAR (pixel: 1 m). b) Radial topographic profiles on the paleofan showing that the latter may have been uplifted by several tens of meters. Vertical exaggeration: 5. The colors of topographic profiles are the same as the lines locating them in a).

23
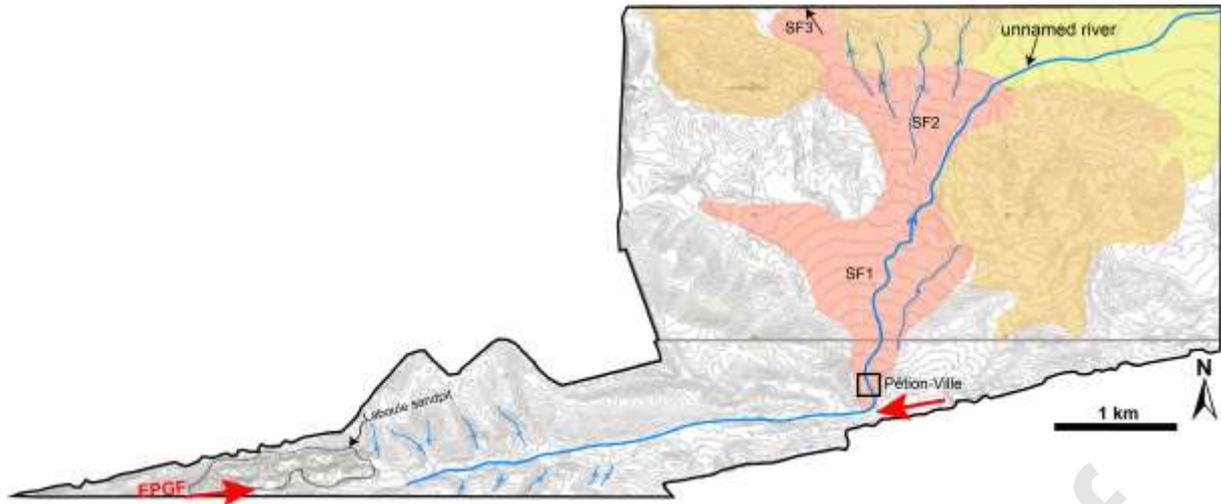
Figure 11: Geomorphic relationship between the unnamed river mapped on Fig. 3 and the EPGF. The river is controlled by the EPGF and flows eastward along the fault trace and bends northward from the apex of PaP paleofan (near Pétion-Ville). The geologic information is the same as in Fig. 10. Topographic contour interval is 10 m. Topographic data: LIDAR (pixel: 1 m).
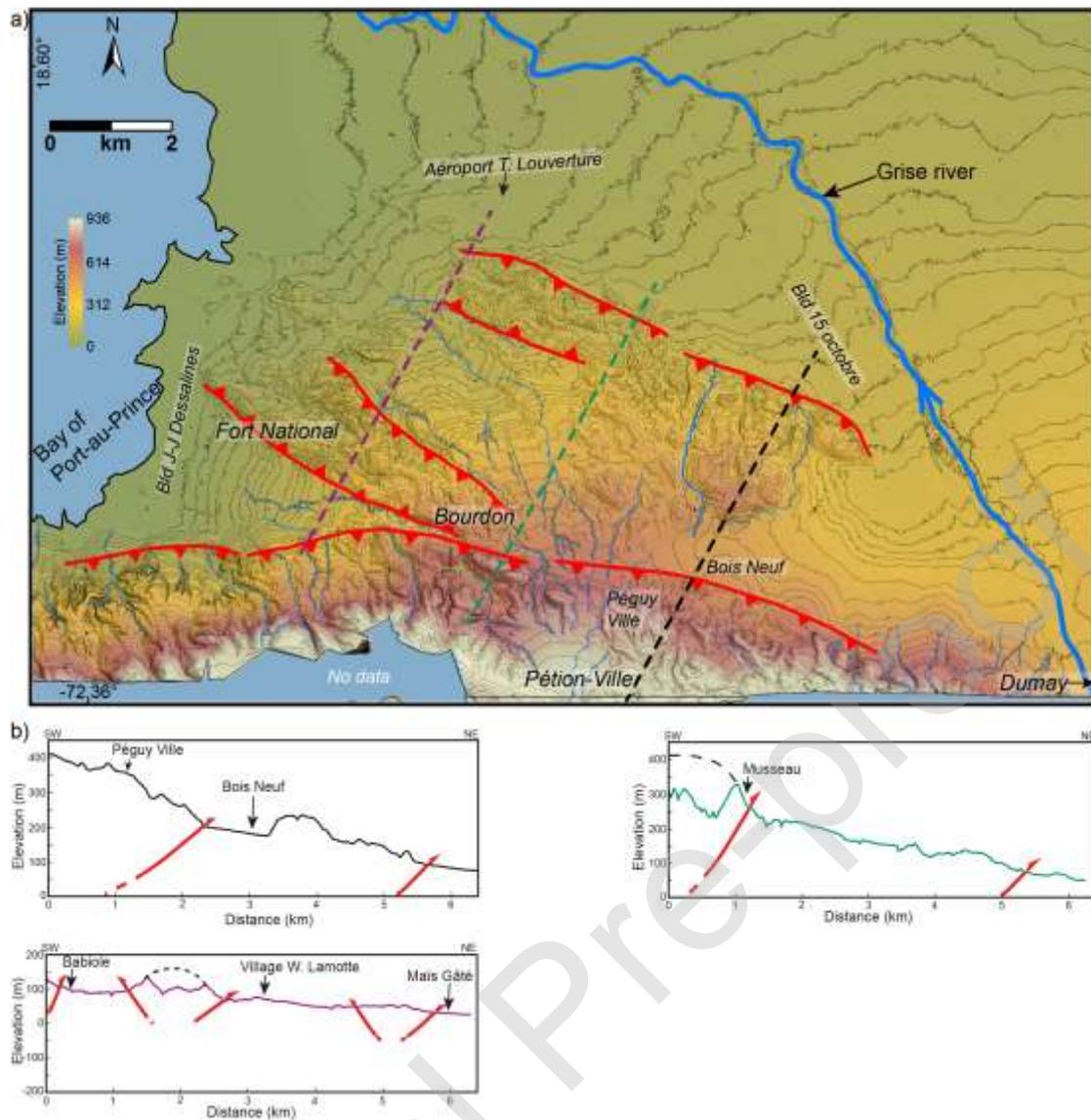
Figure 12: a) Fault mapping in Port-au-Prince showing multiple faults across the paleofan of Port-au-Prince. Topographic contours are 10 m interval. Topographic data: LIDAR (pixel: 1 m). b) Topographic profiles on the paleofan showing the morphology of the structures. Vertical exaggeration: 5. Note that the faults crosscut several significant neighborhoods of Port-au-Prince. The colors of topographic profiles are the same as the lines locating them in a).

Pleisto-Holocene alluvial deposits are shown in bright yellow on Fig. 10a including high-angle fans at mountain fronts [*Cox et al.,* 2011]. The high-angle fans may be explained by high topographic discrepancy between the mountain fronts and the plain in this area (see

topographic profile of Fig. 2b). This Pleisto-Holocene unit is also widely deposited around the paleofan, including within the deep incisions.

The extensive incision of the paleofan, and the hills in particular, may be explained by a scenario of successive variations of the level of the bay of Port-au-Prince. In this case, after the deposition of the paleofan, its related river and channel complex (rills) flowed to the bay. A drop of the level of the bay might force the streams to adjust their incision profiles in order to reach the low sea level. This scenario is consistent with the overall orientation of the incisions on the hill ranges. However, the successive low levels of the bay should have actually been balanced by highstands since its emplacement. In fact, the incisions are so deep that we propose that they have been exacerbated by tectonic uplift. The Pliocene hill ranges described above bear some resemblance to the other young folds identified in the Cul-de-Sac plain, and they may be the result of active folding. Since the borders of the proposed folds are relatively sharp, they may be controlled by bivergent thrusts (Fig. 12a). This suggests that the paleofan is faulted and that active faults cut through several significant neighborhoods of Port-au-Prince (e.g., Bourdon, Fort National, Péguy Ville) (Fig. 12a and b). As the faulting affects the Plio-Pleistocene deposit, the deformation is active after the deposition of this unit.
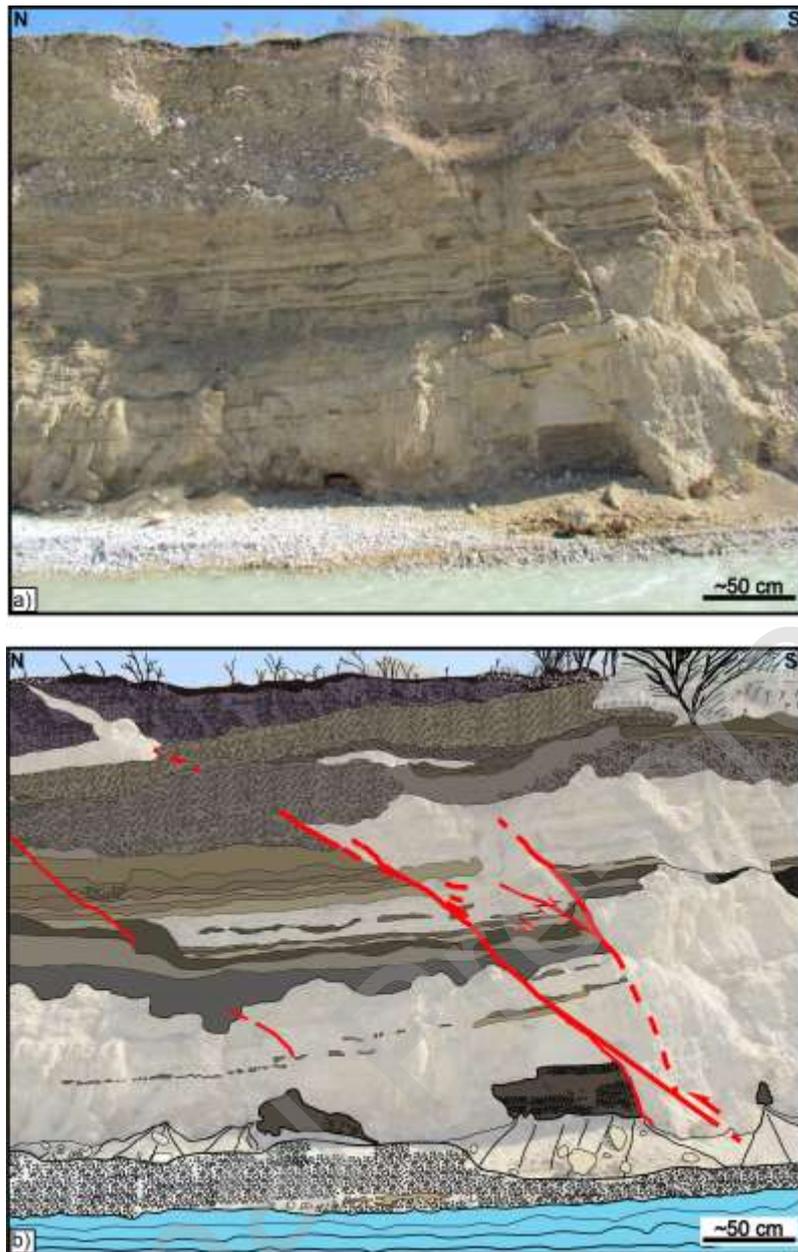
Figure 13: a) and b) Field photograph and interpretation of the exposure of the Dumay Fault on the eastern wall of Grise river (see figure 3 for location). The fault vertically offsets the sedimentary layers by several centimeters. The fault dips at $50 \pm 15°$S.

4.6.- Dumay Fault

The surface of the Grise river fan is smooth with little incision except where it is disturbed by the Nan Cadastre Fold (Supplementary S4). Near the eastern edge of the fan, Holocene sediments seem to be also affected by the Jacquet Fold along which Upper Miocene chalky limestone crops out. To the south of the fan, the EPGF is not well expressed geomorphically and we only recognize the Dumay Fault in the area. In the field, the Dumay Fault is exposed in the eastern cutbank of Grise river (Fig. 13) [*Gold et al.,* 2012; *Saint Fleur et al.,* 2015; This study] where a 10-m-high exposure of fluvial sedimentary deposits reveals several reverse faults. The layers are coarse and thick at the lower and upper part, whereas they are relatively fine and thin in the middle of the wall. The sedimentary layers are offset by several centimeters by several branches of the fault, which dips $50 \pm 15°$ to the south (Fig. 13). The offset is most visible in the middle of the exposure where the layers are the finest and thinnest. However, the main fracture associated with the fault is well seen at the base of the wall. We do not have any evidence that indicates the fault displaces the sediments near the top of the exposure, and there is no scarp on the surface. However, the surface has been used for farming, so it is possible that the fault has displaced the surface and the scarp has been masked by agricultural activities. In addition to the reverse faulting, strike-slip deformation has been observed ~3.2 km west of Dumay (18.50870° / -72.22909°), along a northwest-flowing tributary of the Grise river. Indeed, a fluvial terrace riser was identified and recorded lateral offset of ~6.5 m [*Prentice et al.,* 2010; *Cowgill et al.,* 2012].

5.- Discussion

5.1.- Age constraints for the paleofan of Port-au-Prince

Most of the alluvial fans described here are presumed to be of Quaternary age [*Momplaisir,* 1986]. The only fan that was the subject of a detailed study was the paleofan of Port-au-Prince. Using LIDAR topographic data (pixel: 1 m) and field observations, Cox *et al.* (2011) presented a detailed geological map of the PaP paleofan. Although they did not carry out any absolute dating, they used age estimates for correlative regional map units and landscape analysis from field observations. They also combined their dataset with the response of different soil and bedrock layers to the seismic waves recorded during the 2010 earthquake [*Cox et al.,* 2011]. They estimated the bulk of the sediments of the paleofan to be of Pliocene age (Fig. 10a). Van Den Berghe (1983) observed that the paleofan was deposited on an 80-m-thick marl layer that is rich in planktonic foraminifera such as *Globorotalia margaritae*, characteristic of the Early Pliocene period [*Bolli and Bermúdez,* 1965]. Because they overlie this marl, one can infer that the older fanglomerates of the paleofan are of Early-Middle Pliocene age at most.

The variation in hurricane strength could be a cause for variable river behaviour with time. Using especially alkenone and Mg/Ca ratio proxies, it is well documented that the Early Pliocene was 4°C warmer than today [*Brierley and Fedorov,* 2010; *Fedorov et al.,* 2013], and Middle Pliocene was 2-3°C warmer than today [*Brierley et al.,* 2009; *Dowsett and Robinson,* 2009; *Dowsett et al.,* 1999; *Haywood and Valdes,* 2004; Thompson and Fleming, 1996]. Such temperatures might have corresponded to greenhouse conditions [*Brierley et al.,* 2009], and thus led to more tropical storms or cyclones in the Early-Middle Pliocene than today. These hurricanes might have been more frequent and stronger in the Caribbean [*Fedorov et al.,* 2010]. Thus, the climatic conditions in the Early-Middle Pliocene time might have been favorable for high rates of erosion and deposition during the formation of the paleofan of Port-au-Prince, the biggest fan of the Cul-de-Sac plain. The other fans in the plain, as they are assumed to be

29

younger, their corresponding catchments might have not experienced the same favorable conditions as the corresponding catchment of the paleofan for sedimentary deposition.

5.2.- Offset timing and slip rate

By considering that the paleofan of Port-au-Prince is of Pliocene age, its offset of 7.9 ± 0.3 km is necessarily posterior. We propose three hypotheses (H) for the timing of the offset of the paleofan (Fig. 14):

H1) the offset might have begun since the Pliocene shortly after deposition of the Pliocene fanglomarates. This implies that the inset Plio-Pleistocene fan (SF1-SF3, Fig. 10a) was formed while the strike-slip faulting was active. Then, the overall paleofan was folded (after the offset) (Fig. 14).
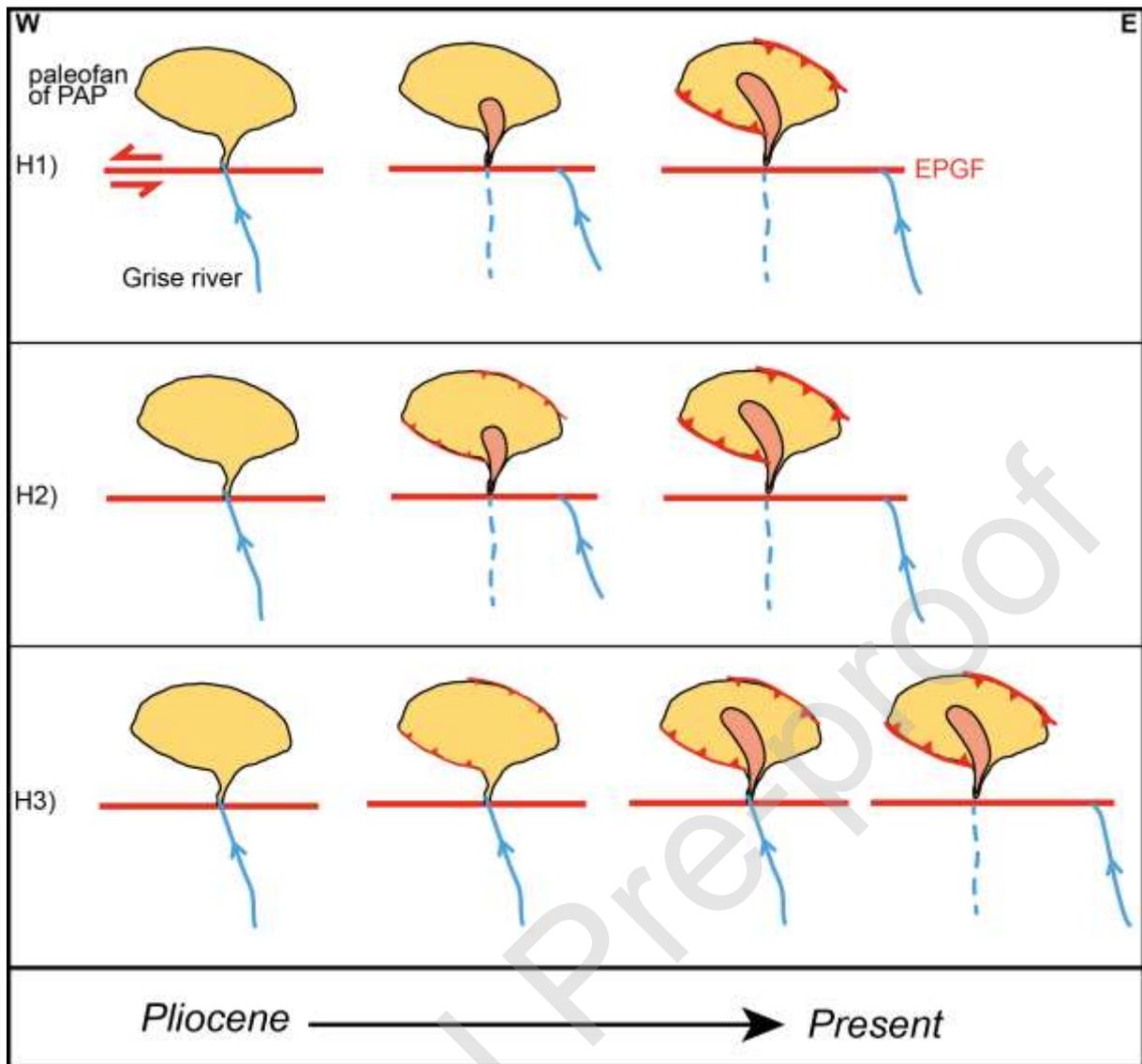
Figure 14: Sketch showing our three different hypotheses (H1-H3) on the timing of the offset of the paleofan of Port-au-Prince (see text for discussion). Yellow area: Pliocene fanglomerates; pinkish area: Plio-Pleistocene fan. The dotted blue line indicates that it is possible that the Plio-Pleistocene fan was deposited by another river other than the Grise river.

H2) the offset began after the deposition of the Pliocene fanglomerates, and the inset Plio-Pleistocene surface was formed during the offset. But, the folding was also active during the offset.

31

H3) the Pliocene fanglomerates were deposited, then folded without being left-laterally offset. The inset Plio-Pleistocene fan was deposited afterward, while the folding continued. Then, the overall paleofan started to be offset.

(H1) implies that the Pliocene paleofan and the younger inset Plio-Pleistocene fan would have been folded by the same amount. However, the Pliocene fanglomerates are much higher and more incised than the inset Plio-Pleistocene fan, suggesting that they are more deformed. According to (H2), the offset would have initiated at the Pliocene (~5.3-2.6 Myr BP). In this case, the horizontal slip rate would be 1.4-3.2 mm/yr. According to (H3), the paleofan was in front of Grise river after the formation of the inset Plio-Pleistocene fan. In this case the offset of the paleofan of Port-au-Prince would be, at most, of Pleistocene age, younger than ~2.6 Myr (following the International Stratigraphic Chart [*Gradstein et al.,* 2004; *Ogg et al.,* 2008]). This implies a minimum slip rate of ~3 mm/yr.

Westward, the EPGF offsets by 40 ± 10 km Lower Miocene folds (Massif de la Selle, Massif de la Hotte) implying that the fault is younger than 15 Myr at this place [*Saint Fleur and Klinger*, under review; *Saint Fleur,* 2014]. This would imply a minimum slip rate of 2-3 mm/yr.

These rates are comparable to those estimated using GPS data: 6 ± 2 mm/yr near Port-au-Prince [e.g., *Symithe and Calais,* 2016]. Indeed, because the geologic rate is a minimum, and the offset age of the fan could be as young as 1 Myr and still be Pleistocene, the geologic and geodetic rates are not much different. Also, given the error on the geodetic rate, it could be as low as 4 mm/yr, not much different from a minimum geologic rate of 3 mm/yr.

5.3. Relevance of the observed deformation

The active folds mapped here are characterized by low hills in the Cul-de-Sac – Enriquillo trough and mainly disturb the topography of alluvial fans associated with north- or

south-flowing rivers. The topography created by the deposition of the fans is characterized by gentle slopes oriented N-S, while hills that disrupt the fans have abrupt slopes that are oriented ~N115°E, oblique to the fans. Thus, it is unlikely that the hills were formed by depositional processes associated with the fans. Moreover, we have shown that the hills are linear and higher (up to 260 m above sea level) than the fans. The existence of wind gaps, uplifted alluvial terraces, ponded sediments, tilted Quaternary beds, and the youthful morphology of the hills are the result of active folding in the Cul-de-Sac plain. These Quaternary folds are located near the eastern tip of the Enriquillo-Plantain Garden Fault (EPGF). They strike parallel to the other folds belonging to the Trans-Haitian Belt and belong to the same system.

To the west of Port-au-Prince, Saint Fleur *et al.* (2015) have recently shown the existence of the Lamentin fold and thrust, and the latter are connected to the EPGF. Momplaisir (1986) also showed the existence of the Trois-Baies Fault that might be connected to the EPGF. We thus suggest that the folds along the northern margin of the Massif de la Selle correspond to blind thrusts connected to the EPGF. But, the EPGF is not geomorphically well expressed in this area where the deformation is distributed between strike-slip and thrust faults. The ~50° south-dipping Dumay Fault, for example, which does not show significant vertical offset in the field (Fig. 13) may have a significant component of strike-slip near the eastern end of the EPGF [Prentice *et al.,* 2010; Cowgill *et al.,* 2012]. We propose that the transpressive N95-100°E Dumay Fault marks a transition between the Léogâne – Pétion-Ville shear zone and the Bahoruco Fault (Fig. 15). Indeed, the fault system undergoes another significant azimuth change along the Bahoruco Fault, which is ~N130°E-striking and accommodates reverse motion. The Dumay and Bahoruco faults, along with the young thrusts in the Cul-de-Sac – Enriquillo plain and the Southern Hispaniola Fault, contribute to maintain the present-day uplift of the Massif de la Selle – Bahoruco Mountain Range (Fig. 15); this is consistent with the highest elevations (e.g., Pic La Selle) bordered by these faults.

33

5.4. Implications for Seismic Hazard

The 2010 Haiti earthquake revealed the complexity of fault systems in southern Hispaniola. Wang *et al.,* (2018) found both evidence for strike-slip and reverse faulting in southern Azuéï Lake. The strike-slip fault is deeply buried and less active than the thrust cutting the lake bed [Wang *et al.,* 2018]. This is consistent with the lack of geomorphic expression of the EPGF in the area and may indicate that Holocene activities are provided by the transpressive Dumay Fault, the Bahoruco Fault and the young thrusts along the Cul-de-Sac – Enriquillo plain. From a kinematic point of view, the EPGF system changes from a significant shear zone at Pétion-Ville, at the apex of PaP paleofan, to accommodate transpression and mainly compression to the east of Port-au-Prince, representing a high seismic hazard. The young folds and thrusts in the Cul-de-Sac – Enriquillo trough show two families. A north-dipping one connected to the Matheux-Neiba Fault zone and a south-dipping one aligning to the south and connected to the Enriquillo-Dumay-Bahoruco fault zone (Fig. 15). We propose that the two families form two distinct deformation fronts in the Cul-de-Sac – Enriquillo trough, consistent with the suturing of the northern island-arc structures and the oceanic plateau terrane of the southern peninsula [Mann *et al.,* 1991]. Thus, the Cul-de-Sac – Enriquillo trough represents a significant seismic hazard for the two capital cities, Port-au-Prince and Santo Domingo.
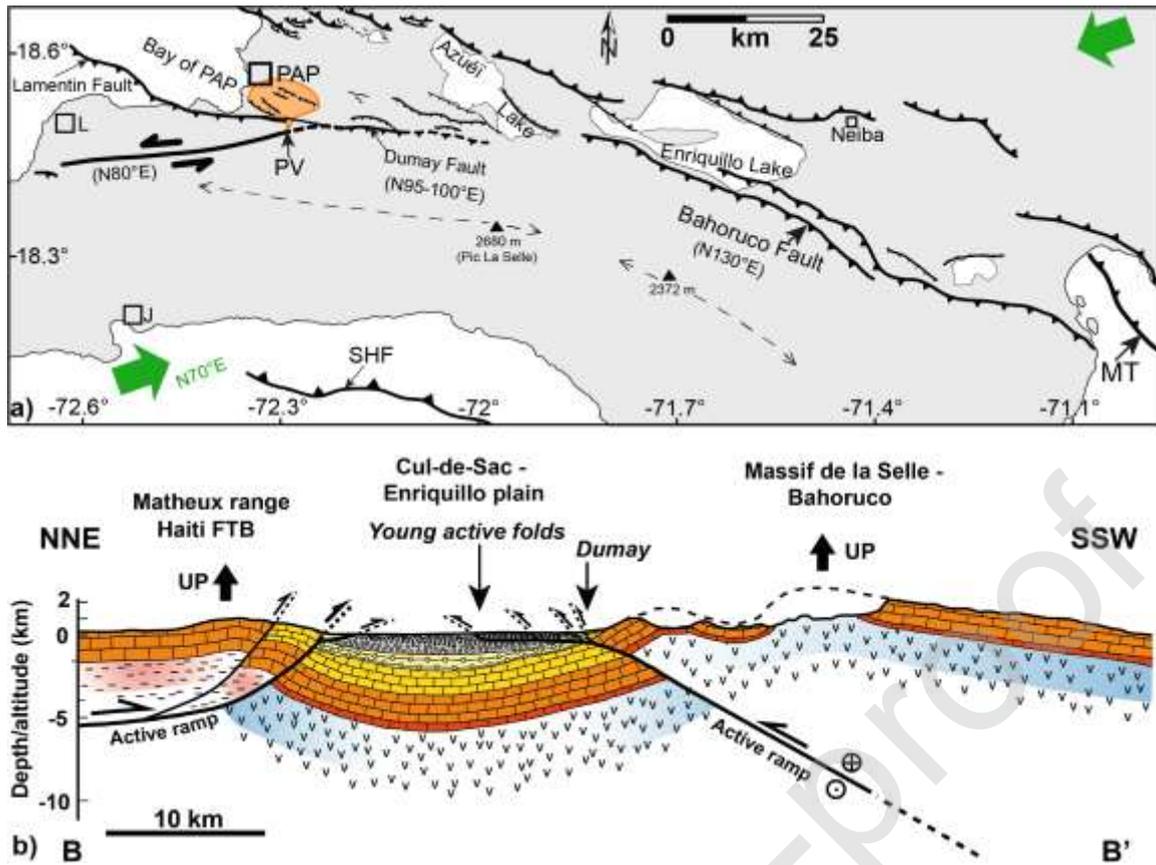
Figure 15: Fault kinematics in southern Hispaniola. Near Port-au-Prince, the deformation is partitioned between strike-slip and reverse faults. The Dumay Fault is transpressive and the Bahoruco Fault is compressive. The green arrows represent the boundary conditions, that is, the oblique convergence between North American and Caribbean plates. Orange shaded is the paleofan of Port-au-Prince. L: Léogâne; J: Jacmel; PAP: Port-au-Prince; PV: Pétion-Ville; EPGF: Enriquillo-Plantain Garden Fault; SHF: Southern Hispaniola Fault; MT: Muertos Trench. b) Overall structural section showing the style of deformation (see Fig. 2 for location). FTB: Fault and Trust Belt.

6. Conclusions

In this study we have, in a first part, acquired morphometric data for six fans and their associated drainage basins along the northern piedmont of the Massif de la Selle. These data revealed that the paleofan of Port-au-Prince is not facing its initial source. Our dataset has shown that the drainage basins have areas up to ~9 times larger than their related fan areas, compatible with the empirical law linking drainage basin and fan areas [*Bull*, 1962; 1977]. The only exception

35

is Port-au-Prince, which present-day drainage basin is ~5.5 times smaller than its paleofan. We inferred that the paleofan was displaced by 7.9 km by the Enriquillo fault from its original drainage basin. This offset implies a minimum slip rate of ~3 mm/yr.

In a second part, we have shown evidence for active folding characterized by low hills in the Cul-de-Sac – Enriquillo trough. In particular, many of those folds have been mapped using high-resolution geospatial data and field observations. The folds mainly disturb the topography of alluvial fans. Those folds and thrusts are connected to the Enriquillo-Dumay-Bahoruco fault zone.

In addition to the strike-slip deformation, the young thrusts documented in Port-au-Prince and in the Cul-de-Sac plain are similar to the Lamentin fault. Port-au-Prince is thus threatened by the 2010-earthquake type, involving both strike-slip and reverse faulting [*Saint Fleur et al.,* 2015; *Rodriguez et al.,* 2018]. These two structure families result from the oblique tectonic context of compression between the rigid Bahamas bank on the North American plate and the Caribbean plate. The deformation related to the oblique compression is actually partitioned between structures accommodating preferably the compressional component of the motion, that is, the numerous folds and thrusts that we have identified, and structures that accommodate the lateral motion, such as the Septentrional Fault and the EPGF. In particular, the young active thrusts in the Cul-de-Sac plain deserve further tectonic investigations in terms of fieldwork, balanced cross-section, together with dating in order to constrain their shortening rate in the direct vicinity of Port-au-Prince.

Declaration of interests

The authors declare that they have no known competing financial interests or personal relationships that could have appeared to influence the work reported in this paper.

Acknowledgments

References

Ali, S. T., A. M. Freed, E. Calais, D. M. Manaker, and W. R. McCann (2008), Coulomb stress evolution in Northeastern Caribbean over the past 250 years due to coseismic, postseismic and interseismic deformation, *Geophysical Journal International*, *174*(3), 904-918.

Bakun, W. H., C. H. Flores, and U. S. ten Brink (2012), Significant Earthquakes on the Enriquillo Fault System, Hispaniola, 1500-2010: Implications for Seismic Hazard, *Bulletin of the Seismological Society of America*, *102*(1), 18-30.

Benford, B., C. DeMets, and E. Calais (2012), GPS estimates of microplate motions, northern Caribbean: evidence for a Hispaniola microplate and implications for earthquake hazard, *Geophysical Journal International*, *191*(2), 481-490.

Bilham, R. (2010), Structural geology: Invisible faults under shaky ground, *Nature Geoscience*, *3*(11), 743-745.

Bolli, H. M., and P. J. Bermúdez (1965), *Zonation based on planktonic foraminifera of Middle Miocene to Pliocene warm-water sediments*, 29 pp., Boletin Informativo / Asociación Venezolana de Geología Mineria y Petroleo.

Brierley, and A. V. Fedorov (2010), Relative importance of meridional and zonal sea surface temperature gradients for the onset of the ice ages and Pliocene- Pleistocene climate evolution, *Paleoceanography*, *25*(2).

Brierley, A. V. Fedorov, Z. Liu, T. D. Herbert, K. T. Lawrence, and J. P. LaRiviere (2009), Greatly expanded tropical warm pool and weakened Hadley circulation in the early Pliocene, *Science*, *323*(5922), 1714-1718.

Briggs, R. W., C. S. Prentice, A. J. Crone, R. D. Gold, K. W. Hudnut, and R. Narcisse (2012), Late Quaternary Blind Thrust Faults along the Southern Margin of the Cul-de-Sac Plain, Haiti: A Newly Recognized Seismic Source?, *AGU Fall Meeting*.

Bull, W. B. (1962), Relation of textural (CM) patterns to depositional environment of alluvial-fan deposits, *Journal of Sedimentary Research*, *32*(2).

Bull, W. B. (1977), The alluvial-fan environment, *Progress in Physical Geography*, *1*(2), 222-270.

Calais, E., and B. Mercier de Lépinay (1995), Strike-slip tectonic processes in the northern Caribbean between Cuba and Hispaniola (Windward Passage), *Marine Geophysical Researches*, *17*(1), 63-95.

Calais, E., A. Freed, G. Mattioli, F. Amelung, S. Jónsson, P. Jansma, S.-H. Hong, T. Dixon, C. Prépetit, and R. Momplaisir (2010), Transpressional rupture of an unmapped fault during the 2010 Haiti earthquake, *Nature Geoscience*, *3*(11), 794-799.

Calmus, T. (1983). Contribution à l'étude géologique du massif de Macaya(sud-ouest d'Haïti, Grandes ACalmusntilles): sa place dans l'évolution de l'orogène Nord-Caraïbe (Doctoral dissertation).

Calmus, and J. M. Vila (1988), The Massif of Macaya (Haiti): the evolution of a Laramide structure in the left-handed-strike-slip boundary between North-America and Caribbean Plates, *Bol. Depto. Geol. Uni-Son,*, *5*, 63-69.

Cooper, J. C. (1983), Geology of the Fondo Negro region, Dominican Republic, State University of New York at Albany. Department of Geological Sciences.

Cowgill, E., Bernardin, T. S., Oskin, M. E., Bowles, C., Yıkılmaz, M. B., Kreylos, O., ... & Bawden, G. W. (2012). Interactive terrain visualization enables virtual field work during rapid scientific response to the 2010 Haiti earthquake. *Geosphere*, *8*(4), 787-804.

Cox, B. R., J. Bachhuber, E. Rathje, C. M. Wood, R. Dulberg, A. Kottke, R. A. Green, and S. M. Olson (2011), Shear wave velocity-and geology-based seismic microzonation of Port-au-Prince, Haiti, *Earthquake Spectra*, *27*(S1), S67-S92.

DeMets, C., R. G. Gordon, and D. F. Argus (2010), Geologically current plate motions, *Geophysical Journal International*, *181*(1), 1-80.

de St-Méry, M. (1803). Description topographique, physique, civile, politique et historique de Saint-Domingue. Philadelphie, 1797. *La danse. Parme*

Dixon, T. H., F. Farina, C. Demets, P. Jansma, P. Mann, and E. Calais (1998), Relative motion between the Caribbean and North American plates and related boundary zone deformation, *JOURNAL OF GEOPHYSIC RESEARCH*, *103*, 15,157-115,182.

Dolan, J. F., Mullins, H. T., Wald, D. J., & Mann, P. (1998). Active tectonics of the north-central Caribbean: Oblique collision, strain partitioning, and opposing subducted slabs. *Special Papers-Geological Society of America*, 1-62.

Douilly, R., Haase, J. S., Ellsworth, W. L., Bouin, M. P., Calais, E., Symithe, S. J., ... & Meremonte, M. E. (2013). Crustal structure and fault geometry of the 2010 Haiti earthquake from temporary seismometer deployments. *Bulletin of the Seismological Society of America*, *103*(4), 2305-2325.

Dowsett, and M. M. Robinson (2009), Mid-Pliocene equatorial Pacific sea surface temperature reconstruction: a multi-proxy perspective, *Philosophical Transactions of the Royal Society A: Mathematical, Physical and Engineering Sciences*, *367*(1886), 109-125.

Dowsett, J. A. Barron, R. Z. Poore, R. S. Thompson, T. M. Cronin, S. E. Ishman, D. A. Willard, and J. A. Barren (1999), Middle Pliocene paleoenvironmental reconstruction: PRISM2. USGS Open File Report.

Fedorov, C. M. Brierley, and K. Emanuel (2010), Tropical cyclones and permanent El Niño in the early Pliocene epoch, *Nature*, *463*(7284), 1066-1070.

Fedorov, C. Brierley, K. Lawrence, Z. Liu, P. Dekens, and A. Ravelo (2013), Patterns and mechanisms of early Pliocene warmth, *Nature*, *496*(7443), 43-49.

Feuillet, N. (2000). *Sismotectonique des Petites Antilles: Liaison entre activité sismique et volcanique* (Doctoral dissertation, Paris 7).

Fraser, G. S., and P. G. DeCelles (1992), Geomorphic controls on sediment accumulation at margins of foreland basins, *Basin Research*, *4*(3-4), 233-252.

Giles, P. T. (2010), Investigating the use of alluvial fan volume to represent fan size in morphometric studies, *Geomorphology*, *121*(3), 317-328.

Gold, R. D., C. S. Prentice, A. J. Crone, R. W. Briggs, and R. Narcisse (2012), Evidence of multiple, prehistoric, ground-rupturing earthquakes along the Enriquillo-Plantain Garden Fault system near Port-au-Prince, Haiti, paper presented at AGU Fall Meeting Abstracts.

Gradstein, F. M., J. G. Ogg, and A. G. Smith (2004), *A geologic time scale 2004*, Cambridge University Press.

Guérit, L. (2014), Caractéristiques morpho-sédimentaires des cônes alluviaux et reconstitution de leurs paléo-flux d'eau et de sédiments. Exemples naturels du piedmont nord du Tian Shan (Xinjiang, Chine) et modélisation expérimentale, 266 pp, Université Paris Diderot (Paris 7).

Harvey (1997), The role of alluvial fans in arid zone fluvial systems, *Arid zone geomorphology (2nd edition). John Wiley & Sons*, 231-260.

Hayes, G., R. Briggs, A. Sladen, E. Fielding, C. Prentice, K. Hudnut, P. Mann, F. Taylor, A. Crone, and R. Gold (2010), Complex rupture during the 12 January 2010 Haiti earthquake, *Nature Geoscience*, *3*(11), 800-805.

Haywood, A. M., and P. J. Valdes (2004), Modelling Pliocene warmth: contribution of atmosphere, oceans and cryosphere, *Earth and Planetary Science Letters*, *218*(3), 363-377.

Hubert-Ferrari, A., J. Suppe, R. Gonzalez-Mieres, and X. Wang (2007), Mechanisms of active folding of the landscape (southern Tian Shan, China), J. Geophys. Res.,112, B03S09, doi:10.1029/2006JB004362.

Lacassin, R., Klinger, Y., & Feuillet, N. (2013). Sismotectonique du tremblement de terre du 12 janvier 2010 en Haïti. *Outre-terre*, (1), 163-183.

Manaker, D. M., E. Calais, A. M. Freed, S. T. Ali, P. Przybylski, G. Mattioli, P. Jansma, C. Prépetit, and J. B. de Chabalier (2008), Interseismic Plate coupling and strain partitioning in the Northeastern Caribbean, *Geophysical Journal International*, *174*(3), 889-903.

Mann, P., K. Burke, and T. Matumoto (1984), Neotectonics of Hispaniola: plate motion, sedimentation, and seismicity at a restraining bend, *Earth and Planetary Science Letters*, *70*, 311-324.

Mann, P., P. McLaughlin, and C. Cooper (1991), Geology of the Azua and Enriquillo basins, Dominican Republic; 2, Structure and tectonics, *Geological Society of America Special Papers*, *262*, 367-390.

43

Mann, P., F. W. Taylor, R. L. Edwards, and T.-L. Ku (1995), Actively evolving microplate formation by oblique collision and sideways motion along strike-slip faults: An example from the northeastern Caribbean plate margin, *Tectonophysics*, *246*, 1-69.

Mann, P., E. Calais, J.-C. Ruegg, C. DeMets, P. E. Jansma, and G. S. Mattioli (2002), Oblique collision in the northeastern Caribbean from GPS measurements and geological observations, *Tectonics*, *21*(6), 7-1-7-26.

Mather, A., A. Harvey, and M. Stokes (2000), Quantifying long-term catchment changes of alluvial fan systems, *Geological Society of America Bulletin*, *112*(12), 1825-1833.

McCann, W. R. (2006), *Estimating the threat of tsunamogenic earthquakes and earthquake induced-landslide tsunami in the Caribbean*, World Scientific Publishing, Singapore.

Mercier de Lépinay, et al. (2011), The 2010 Haiti earthquake: A complex fault pattern constrained by seismologic and tectonic observations, *Geophysical Research Letters*, *38*(22).

Momplaisir, R., & Boisson, D. (1988). Carte Géologique de la République d'Haiti, South-East sheet (Port-au-Prince). *BME*.

Momplaisir, R. B. A. (1986). Contribution a l'Etude Geologique de la partie orientale du massif de la hotte (presqu'ile de sud d'Haiti): synthese structurale des marges de la presqu'ile a partir de donnees sismiques (Doctoral dissertation, Ph. D. thesis).

Nettles, M., and V. Hjörleifsdóttir (2010), Earthquake source parameters for the 2010 January Haiti main shock and aftershock sequence, *Geophysical Journal International*, *183*(1), 375-380.

Ogg, J. G., G. Ogg, and F. M. Gradstein (2008), *The concise geologic time scale*.

Pindell, J. L., S. C. Cande, W. C. Pitman III, D. B. Rowley, J. F. Dewey, J. Labrecque, and W. Haxby (1988), A plate-kinematic framework for models of Caribbean evolution, *Tectonophysics*, *155*, 121-138.

Prentice, C., P. Mann, L. R. Peña, and G. Burr (2003), Slip rate and earthquake recurrence along the central Septentrional fault, North American–Caribbean plate boundary, Dominican Republic, *Journal of Geophysical Research*, *108*(B3).

Prentice, C., P. Mann, A. J. Crone, R. D. Gold, K. W. Hudnut, R. W. Briggs, R. D. Koehler, and P. Jean (2010), Seismic hazard of the Enriquillo–Plantain Garden fault in Haiti inferred from palaeoseismology, *Nature Geoscience*, *3*, 789-793.

Pubellier, M., J. M. Vila, and D. Boisson (1991), North Caribbean neotectonic events: The Trans-Haitian fault system. Tertiary record of an oblique transcurrent shear zone uplifted in Hispaniola, *Tectonophysics*, *194*, 217-236.

Pubellier, M., A. Mauffret, S. Leroy, J. M. Vila, and H. Amilcar (2000), Plate boundary readjustment in oblique convergence: Example of the Neogene of Hispaniola, Greater Antilles, *Tectonics*, *19*(4), 630-648.

45

Rodriguez, J., Havskov, J., Sørensen, M. B., & Santos, L. F. (2018). Seismotectonics of south-west Dominican Republic using recent data. *Journal of Seismology*, 1-14.

Saint Fleur, N., & Klinger, Y. (under review). Detailed map, displacement, paleoseismology, and segmentation of the Enriquillo-Plantain Garden Fault in Haiti.

Saint Fleur, N., Feuillet, N., Grandin, R., Jacques, E., Weil- Accardo, J., & Klinger, Y. (2015). Seismotectonics of southern Haiti: A new faulting model for the 12 January 2010 M7. 0 earthquake. *Geophysical Research Letters*, *42*(23), 10-273.

Saint Fleur, N. (2014). Sismotectonique du système de failles d'Enriquillo et du séisme du 12 janvier 2010 (M7.0) en Haïti (Doctoral dissertation, Ph. D. thesis).

Sykes, L. R., W. R. McCann, and A. L. Kafka (1982), Motion of Caribbean Plate during last 7 million years and implications for earlier Cenozoic movements, *Journal of Geophysical Research*, *87*(B13), 10656.

Symithe, S. J., Calais, E., Haase, J. S., Freed, A. M., & Douilly, R. (2013). Coseismic slip distribution of the 2010 M 7.0 Haiti earthquake and resulting stress changes on regional faults. *Bulletin of the Seismological Society of America*, *103*(4), 2326-2343.

Symithe, S., & Calais, E. (2016). Present-day shortening in Southern Haiti from GPS measurements and implications for seismic hazard. *Tectonophysics*, *679*, 117-124.

Taylor, F., P. Mann, S. Valastro Jr, and K. Burke (1985), Stratigraphy and radiocarbon chronology of a subaerially exposed Holocene coral reef, Dominican Republic, *The Journal of Geology*, *93*, 311-332.

Thompson, R. S., and R. F. Fleming (1996), Middle Pliocene vegetation: reconstructions, paleoclimatic inferences, and boundary conditions for climate modeling, *Marine Micropaleontology*, *27*(1), 27-49.

Toloczyki, M., & Ramirez, I. (1991). Geologic map of the Dominican Republic 1: 250,000. *Ministry of Industry and Commerce, Department of Mining, Geographic Institute of the Univerisity of Santo Domingo.*

Van Den Berghe, B. (1983), Evolution sédimentaire et structurale depuis le Paléocène du secteur massif de la Selle(Haiti) «Baoruco»(République dominicaine)-«nord de la ride de Beata» dans l'orogène nord Caraïbe(Hispaniola-Grandes Antilles).

van den Bold, W. A. (1975), Neogene biostratigraphy (Ostracoda) of southern Hispaniola, *Bull. Am. Paleontol.*, *66*(286), 599-639.

Wang, J., Mann, P., & Stewart, R. R. (2018). Late Holocene structural style and seismicity of highly transpressional faults in southern Haiti. *Tectonics*, *37*(10), 3834-3852.

Weissmann, G. S., and G. E. Fogg (1999), Multi-scale alluvial fan heterogeneity modeled with transition probability geostatistics in a sequence stratigraphic framework, *Journal of Hydrology*, *226*(1), 48-65.

47

Wessels, R. J., Ellouz-Zimmermann, N., Bellahsen, N., Hamon, Y., Rosenberg, C., Deschamps, R., ... & Leroy, S. (2019). Polyphase tectonic history of the Southern Peninsula, Haiti: from folding-and-thrusting to transpressive strike-slip. *Tectonophysics*, *751*, 125-149.

Whipple, K. X., and C. R. Trayler (1996), Tectonic control of fan size: the importance of